



# HHS Public Access

Author manuscript

*Am J Ophthalmol.* Author manuscript; available in PMC 2020 November 01.

Published in final edited form as:

*Am J Ophthalmol.* 2019 November ; 207: 99–109. doi:10.1016/j.ajo.2019.05.024.

## Projection-Resolved Optical Coherence Tomography Angiography of the Peripapillary Retina in Glaucoma

Liang Liu, Beth Edmunds, Hana Takusagawa, Shandiz Tehrani, Lorinna Lombardi, John C. Morrison, Yali Jia, David Huang

Casey Eye Institute and Department of Ophthalmology, Oregon Health and Science University, Portland, Oregon, USA

### Abstract

**Purpose:** To detect plexus-specific peripapillary retinal perfusion defects in glaucoma using projection-resolved optical coherence tomography (PR-OCTA).

**Design:** Prospective cross-sectional study.

**Methods:** One eye each of 45 perimetric glaucoma participants and 37 age-matched normal participants were scanned using 4.5-mm OCTA scans centered on the disc. The PR-OCTA algorithm removed flow projection artifacts in OCT angiograms. Five *en face* OCTA slabs were analyzed: nerve fiber layer plexus (NFLP), ganglion cell layer plexus (GCLP), superficial vascular complex (SVC = NFLP + GCLP), deep vascular complex (DVC), and all plexuses combined. Peripapillary retinal capillary density (CD) and vessel density (VD) were calculated using a reflectance-compensated algorithm.

**Results:** Focal capillary dropout could be visualized more clearly in the NFLP than the other slabs. The NFLP, SVC and all-plexus CD in the glaucoma group were significantly lower ( $P < 0.001$ ) than the normal group, but no significant differences in GCLP-CD and DVC-CD appeared between the two groups. Both NFLP-CD and SVC-CD had excellent diagnostic accuracy as measured by the area under the receiver operating characteristic curve (AROC=0.981 and 0.976), correlation with visual field mean deviation (Pearson  $r = 0.819$  and  $0.831$ ), and repeatability (intraclass correlation coefficient = 0.947 and 0.942). Performances of NFLP-VD and SVC-VD were similar to the corresponding CD parameters.

---

**Correspondence and reprint requests to:** David Huang, MD, PhD davidhuang@alum.mit.edu, Peterson Professor of Ophthalmology & Professor of Biomedical Engineering, Casey Eye Institute, Oregon Health & Science University, 3375 S.W. Terwilliger Blvd. Portland, OR 97239-4197, Phone (503) 4945131.

**ClinicalTrials.gov information: Identifier:** ; **Responsible party:** David Huang, Oregon Health and Science University; **Official title:** Longitudinal Observational Study Using Functional and Structural Optical Coherence Tomography to Diagnose and Guide Treatment of Glaucoma

#### Financial Disclosure

OHSU, Yali Jia, and David Huang have financial interest in Optovue, Inc., a company that may have a commercial interest in the results of this research and technology. These potential conflicts of interest have been reviewed and are managed by OHSU. The other authors do not report any potential financial conflicts of interest.

**Publisher's Disclaimer:** This is a PDF file of an unedited manuscript that has been accepted for publication. As a service to our customers we are providing this early version of the manuscript. The manuscript will undergo copyediting, typesetting, and review of the resulting proof before it is published in its final citable form. Please note that during the production process errors may be discovered which could affect the content, and all legal disclaimers that apply to the journal pertain.

**Conclusions:** In this glaucoma group, reduction in perfusion was more pronounced in superficial layers of the peripapillary retina (NFLP and SVC) than the deeper layers. Reflectance-compensated CD and VD parameters for both NFLP and SVC could be useful in the clinical management of glaucoma.

---

## Introduction

Glaucoma is the second leading cause of blindness in the world and a major source of morbidity and disability in the United States.<sup>1-4</sup> Optical coherence tomography (OCT) of the optic disc,<sup>5,6</sup> peripapillary retinal nerve fiber layer (NFL),<sup>6-8</sup> and macular ganglion cell structures<sup>8-12</sup> has provided precise objective measurements for the diagnosis and monitoring of glaucoma. However, structural OCT has significant limitations. Structural OCT cannot detect the earliest stages of glaucoma, when ganglion cells may be dysfunctional but have not yet died and led to loss of tissue thickness. In the later stages, residual scar tissue provides a floor to NFL and ganglion cell related tissue thickness, thus limiting the usefulness of structural OCT in monitoring advanced glaucoma.<sup>13-15</sup> This limited dynamic range of structural changes also manifests as poor correlation between structural OCT parameters and visual field (VF) parameters<sup>13, 16, 17</sup>.

Several years ago we introduced OCT angiography (OCTA) as a further refinement of OCT in glaucoma evaluation.<sup>18-21</sup> Glaucoma has been shown to reduce vessel density (VD) in the optic disc,<sup>20</sup> peripapillary retina,<sup>21-24</sup> and macular retina.<sup>25, 26</sup> OCTA VD parameters show less floor effect and better correlation with VF parameters.<sup>14, 21</sup> These early encouraging results show that OCTA has the potential to complement VF and structural OCT in the assessment of glaucoma damage.

OCTA is a rapidly advancing technology and its optimal use in glaucoma management is still being explored. Several recent investigators have focused on the peripapillary nerve fiber layer plexus (NFLP, also known as the radial peripapillary capillaries). However, it is not clear how glaucoma damages deeper vascular plexuses at the peripapillary retina. One technical difficulty that prevented plexus-specific analysis of the retinal circulation is that the flow projection artifact<sup>12, 27</sup> projects superficial vascular patterns onto the deeper layers, making it impossible to cleanly quantify the vessel density in deeper vascular plexuses. Our group has developed a projection-resolved optical coherence tomographic angiography (PR-OCTA) algorithm to effectively remove the projection artifact and provide clean angiograms of deeper vascular plexuses.<sup>12, 28, 29</sup> Recently, we used the PR-OCTA algorithm to show the superficial vascular complex (SVC) to be the best slab to detect glaucomatous changes in the macular region.<sup>25</sup> In this paper, we examine the performance of the PR-OCTA algorithm in the peripapillary region to answer the question whether the NFLP might be the peripapillary retinal plexus of choice in glaucoma evaluation. In addition, we also investigate whether capillary density (CD), which is VD minus the larger retinal vessels, provides advantages over VD in either diagnostic accuracy or measurement precision.

## Methods

### Study Population

This prospective observation study was performed from March 6, 2015 to May 31, 2017 at the Casey Eye Institute, Oregon Health & Science University (OHSU). The [ClinicalTrials.gov](https://clinicaltrials.gov) identifier number is . The research protocols were approved by the Institutional Review Board at OHSU, and carried out in accordance with the tenets of the Declaration of Helsinki. Written informed consent was obtained from each participant.

All participants were part of the “Functional and Structural Optical Coherence Tomography for Glaucoma” study. The inclusion criteria for the perimetric glaucoma (PG) group were: (1) an optic disc rim defect (thinning or notching) or NFL defect visible on slit-lamp biomicroscopy; and (2) a consistent glaucomatous pattern, on both qualifying Humphrey SITA 24-2 VFs, meeting at least one of the following criteria: pattern standard deviation (PSD) outside normal limits ( $p < 0.05$ ) or glaucoma hemifield test outside normal limits.

For the normal group, the inclusion criteria were: (1) no evidence of retinal pathology or glaucoma; (2) a normal Humphrey 24-2 visual field; (3) intraocular pressure  $< 21$  mm Hg; (4) central corneal pachymetry  $> 500$  microns; (5) no chronic ocular or systemic corticosteroid use; (6) an open angle on gonioscopy; (7) a normal appearing optic nerve head (ONH) and NFL; and (8) symmetric ONH between left and right eyes.

The exclusion criteria for both groups were: (1) best-corrected visual acuity less than 20/40; (2) age  $< 30$  or  $> 80$  years; (3) refractive error of  $> +3.00D$  or  $< -7.00D$ ; (4) previous intraocular surgery except for an uncomplicated cataract extraction with posterior chamber intraocular lens implantation; (5) any diseases that may cause VF loss or optic disc abnormalities; or (6) inability to perform reliably on automated VF testing. One eye from each participant was scanned and analyzed. For normal eyes, the eye was randomly selected. For the glaucoma group, the eye with the worse VF was selected.

### Visual Field Testing

VF tests were performed with the Humphrey Field Analyzer II (Carl Zeiss, Inc.) set for the 24-2 threshold test, size III white stimulus, using the SITA standard algorithm.

### Optical Coherence Tomography

A 70-kHz, 840-nm wavelength spectral-domain OCT system (Avanti RTVue-XR, Optovue Inc.) was used.

### Image Acquisition and Processing

The peripapillary retinal region was scanned using a 4.5×4.5-mm volumetric angiography scan centered on fixation. Each volume was comprised of 304 line-scan locations at which 2 consecutive B-scans were obtained. Each B-scan contained 304 A-scans. The AngioVue software used the SSADA algorithm, which compared the consecutive B-scans at the same location to detect flow using motion contrast.<sup>18</sup> Each scan set was comprised of 2 volumetric scans: 1 vertical-priority raster and 1 horizontal-priority raster. The AngioVue software used

an orthogonal registration algorithm to register the 2 raster volumes to produce a merged 3D OCT angiogram.<sup>30</sup> Two sets of scans were performed within one visit. The OCTA parameters from the two scans were then averaged for further analysis.

The merged volumetric angiograms were then exported for custom processing using the Center for Ophthalmic Optics & Lasers-Angiography Reading Toolkit software.<sup>31</sup> This software removed flow projection artifacts and calculated reflectance-compensated capillary density (CD). The OCTA scans contained both volumetric flow (decorrelation) data as well as structural (reflectance) data. The PR-OCTA algorithm retained flow signal from real blood vessels while suppressing projected flow signal in deeper layers, which appeared as downward tails on cross-sectional angiograms and duplicated vascular patterns on *en face* angiograms.<sup>12, 28, 32</sup> PR-OCTA visualized up to four retinal plexuses: the nerve fiber layer plexus (NFLP), the ganglion cell layer plexus (GCLP), the intermediate capillary plexus (ICP), and the deep capillary plexus (DCP).<sup>28, 33-36</sup> In the peripapillary retina, as the ICP and DCP were often very thin, these were combined to form a single measure, the deep vascular complex (DVC). The PR-OCTA volume was segmented into NFLP, GCLP, SVC (NFLP + GCLP), DVC (ICP + DCP) and all-plexus retina slabs (Figure 1) for VD and CD measurement.<sup>28</sup> Segmentation of the retinal layers was performed by automated MATLAB programs that operate on the structural OCT data. Further manual correction of the segmentation was conducted if required. An *en face* angiogram of each slab was obtained by maximum flow (decorrelation value) projection. The vessel density (VD), defined as the percentage area occupied by the large vessels and microvasculature, was evaluated in the 4×4 mm scan area excluding the central 2mm diameter circle, which was manually centered on the optic disc based on the enface reflectance image. Arterioles and venules (larger vessels) were automatically identified by thresholding the *en face* mean projection of OCT reflectance within the all-plexus slab. After these larger vessels were excluded, the remaining angiogram was used to compute capillary density (CD).

Because we found OCTA measurements to be strongly correlated with signal strength index in previous studies, we developed a reflectance-adjustment method that corrected the artifactually lower flow signal in regions of reduced reflectance (e.g. due to media opacity or pupil vignetting).<sup>37</sup> The method is based on statistical analysis of the relationship between the flow noise in the FAZ with reflectance in retinal tissue, in which the reflectance was manipulated by simulated media opacity (optical filters). In the extrafoveal retina, the average reflectance in the inner nuclear layer, outer plexiform layer, and outer nuclear layers was used to adjust the threshold of flow signal value to classify vessel versus static tissue on *en face* OCTA. Clinical validation showed that this algorithm was able to remove the dependence of retinal OCTA measurements on the signal strength index and reduce population variation.<sup>37</sup>

Image quality was assessed for all OCTA scans. Poor quality scans with signal strength index (SSI) below 50, or registered image sets with residual motion artifacts (discontinuous vessel pattern) were excluded from analysis. Two image sets, each meeting the quality criteria, were required in order to provide data for an assessment of within-visit repeatability. These were then averaged for further analysis. Within-visit repeatability was assessed by the

pooled standard deviation (Pooled SD), the intraclass correlation coefficient (ICC). Population variation was assessed by standard deviation (SD).

### Structural OCT Analysis

The global average NFL thickness was measured from a 3.45mm diameter circular scan centered on the optic disc. The result for each participant was the average value of two sets of imagings obtained at one visit.

### Statistical Analysis

The Student's t test was used to compare normal and glaucoma groups. Pearson correlation was employed to investigate the effect of age, mean ocular perfusion pressure (MOPP), and intraocular pressure (IOP) on CD measurements.  $MOPP = 2/3 * MAP - IOP$ , where mean arterial pressure (MAP) =  $2/3 * \text{diastolic blood pressure} + 1/3 * \text{systolic blood pressure}$ . Pearson correlation was also used to determine the relationships between peripapillary retinal CD and the traditional glaucoma measurements of function and structure, such as the VF mean deviation and circumpapillary retinal nerve fiber layer thickness. The correlation coefficients were also compared.<sup>38</sup> A generalized linear model was used to evaluate the effect of eye drops and systemic medications on the OCTA parameters. A multivariate analysis was used to demonstrate which OCT and OCTA parameters dominate the correlation with VF. The area under the receiver operating characteristic curve (AROC), sensitivity, and specificity were used to evaluate diagnostic accuracy. The estimated sensitivities for fixed specificities were calculated by MedCalc software using the method of Zhou et al.<sup>39</sup> The McNemar test and the method of DeLong et al were used to compare sensitivity and AROC of different parameters.<sup>40</sup> All statistical analyses were performed with SPSS20.0 (SPSS Inc., Chicago, IL) and MedCalc 10.1.3.0 (MedCalc Software, Ostend, Belgium, [www.medcalc.be](http://www.medcalc.be)). The statistical significance was assumed at  $P < 0.05$ . However, for multiple comparisons of OCT and OCTA parameters between normal and glaucoma groups, the Bonferroni correction was applied with resultant significance level set at  $P < 0.008$ .

## Results

### Study Population

Peripapillary retinal perfusion was studied in 37 normal and 45 perimetric glaucoma participants. Three normal and four glaucoma participants were not analyzed due to poor OCTA scan quality – leaving 34 normal and 41 glaucoma participants for statistical analysis. In the glaucoma group, 29 participants had early glaucoma, 11 had moderate glaucoma, and 1 had advanced glaucoma, according to the Hodapp-Parrish-Anderson classification system.<sup>41</sup> All 41 glaucoma patients were using at least one of 4 classes of glaucoma drops (Table 1). Prostaglandin analogs were used in 33 patients; beta-blockers were used in 19 patients; alpha agonists were used in 7 patients; carbonic anhydrase inhibitors were used in 19 patients. There was no significant difference in NFLP or SVC parameters associated with these eye drops. Among the 41 glaucoma patients, 14 patients were using aspirin, 10 patients were using and blood pressure medications. Among the 34 normal participants, 5 participants were using aspirin and 8 participants were using blood pressure medications.

There was no significant difference in NFLP or SVC parameters associated with these glaucoma and systemic medications. There was no statistically significant difference between the normal and glaucoma groups for age, IOP, axial length, MOPP and systolic/diastolic blood pressures (Table 1).

### Qualitative Assessment of Focal Capillary Dropout

In the normal eye (Figure 2), the *en face* PR-OCTA of the NFLP showed that the radial peripapillary capillary density was greater along the superotemporal and inferotemporal arcuate nerve fiber bundles. The SVC showed the same distribution pattern, but because the SVC contained both NFLP and GCLP, the capillary density in the SVC was higher than in the NFLP. A perimetric glaucoma eye was chosen to demonstrate the loss of retinal capillaries in the superotemporal region, in comparison with a normal eye (Figure 2). In the glaucomatous eye, severe capillary dropout in a wedge pattern could be visualized in the NFLP and SVC. The GCLP and All-plexus angiograms also showed decreased capillary density in the same region, but to a lesser degree. No capillary dropout was found in the DVC (Figure 2). Overall, the NFLP slab provided the best contrast for visualizing the focal glaucomatous defect.

### Comparison between PR-OCTA and Non-PR-OCTA

En face non-PR-OCTA images of the deeper slabs (GCLP and DVC) contain projection artifacts from the most superficial slab (NFLP). These projected patterns could be recognized as large vessels and radial capillaries (Figure 3). The non-PR-OCTA DVC angiogram showed projected NFLP perfusion defects in the glaucoma eye (Figure 3). PR-OCTA successfully removed these projection artifacts.

Since the NFLP is the most superficial vascular slab, it does not contain any projection artifacts. Therefore the non-PR-OCTA images appear the same as the PR-OCTA images for this slab.

### Quantitative Assessment of OCTA Parameters

The capillary density in the NFLP, SVC and all-plexus slabs of the glaucomatous eyes were lower than in the normal eyes (all  $P < 0.001$ ). There were no significant differences in the GCLP-CD and DVC-CD between the glaucoma and normal groups (Table 1).

In the normal group, when both age and SSI are included in a multivariate linear regression analysis, the GCLP-CD, DVC-CD and all-plexus-CD were correlated with SSI (scale of 100) and age (years). Higher CD in these slabs were correlated with stronger signal and younger age.

$$\text{GCLP - CD} = -0.16\% \times \text{age} + 0.47\% \times \text{SSI} + 27.1\% \quad (R^2 = 0.63, P = 0.064 \text{ for age and } P < 0.001 \text{ for SSI})$$

$$\text{DVC - CD} = -0.22\% \times \text{age} + 0.87\% \times \text{SSI} + 2.7\% \quad (R^2 = 0.78, P = 0.037 \text{ for age and } P < 0.001 \text{ for SSI})$$

$$\text{All-plexus-CD} = -0.12\% \times \text{age} + 0.30\% \times \text{SSI} + 76.1\% \quad (R^2 = 0.57, P = 0.059 \text{ for age and } P < 0.001 \text{ for SSI}).$$



The NFLP-CD and SVC-CD were not significantly correlated with age or SSI ( $P>0.13$ ). There was no correlation between MOPP or IOP with the CD in any slabs in the normal or glaucoma groups.

### **Repeatability and Population Variation**

In both normal and glaucoma participants (Table 2), the NFLP-CD, SVC-CD, and All-plexus-CD had excellent within-visit repeatability as measured by pooled standard deviation (Pooled SD) and Intraclass correlation coefficient (ICC). They also had tight population variations of less than 5%. In comparison, the GCLP-CD and DVC-CD had worse ICC and wider population variation.

### **Glaucoma Diagnostic Accuracy of Capillary Density and Thickness Parameters**

The NFLP-CD had significantly higher sensitivity among the OCTA parameters (Table 3). Its sensitivity was significantly ( $P=0.016$ ) higher than all-plexus-CD, but not significantly higher when compared to NFL thickness ( $P=0.25$ ). The sensitivity of SVC-CD was close to NFLP-CD, but not significantly higher than all-plexus-CD or NFL thickness ( $P>0.063$ ). The NFLP-CD and SVC-CD AROCs did not differ significantly with all-plexus-CD and NFL thickness AROCs ( $P>0.099$  for all pairwise comparisons). The GCLP-CD and DVC-CD had significantly worse sensitivity and AROC compared to the other parameters.

### **Correlation with Traditional Glaucoma Diagnostic Measurements**

The NFLP-CD, SVC-CD and all-plexus-CD had excellent correlation with the NFL thickness and good correlation with the VF-MD (Table 4, Figure 4). These correlations were highly significant. The NFLP-CD had significantly ( $P<0.02$ ) higher linear correlation with VF-MD than the correlation between NFL thickness with VF-MD, suggesting the visual function is better correlated with perfusion than structure. In the multivariate analysis where the VF-MD was the dependent variable, and the two independent variables were NFLP-CD and NFL thickness, NFLP-CD remain significant ( $P<0.0001$ ), while NFL thickness was no longer significant ( $P=0.92$ ).

### **Comparison of Capillary Density and Vessel Density in OCTA Measurements**

The two slabs with the highest diagnostic power, NFLP and SVC, were used to compare the capillary density and vessel density. The four OCTA measurements, NFLP-CD, NFLP-VD, SVC-CD and SVC-VD, had excellent within-visit repeatability as measured by the pooled SD and ICC in both normal and glaucoma groups (Table 5). All the four measurements had tight population variation, high correlation with VF-MD, and high diagnostic power as measured by AROC. The CD parameters had slightly better AROC than the VD parameters, and the NFLP parameters had slightly better AROC than the SVC parameters, but the differences were not statistically significant.

### **Ganglion Cell Layer Plexus in More Advanced Glaucoma**

We were surprised to find that GCLP-CD was not significantly lower in the glaucoma group compared to the normal group. This might have been because the glaucoma group consisted mostly of patients with mild glaucoma. We therefore further tested the hypothesis that

GCLP-CD was reduced in the combined moderate (11 participants) and advanced (1 participant) glaucoma subgroup. The GCLP-CD was  $46.5 \pm 5.6\%$  in the moderate/advanced glaucoma subgroup (12 participants) and  $49.4 \pm 5.6\%$  in the normal group (34 participants). The difference was of borderline significance ( $p = 0.064$ , one-tailed t-test).

## Discussion

Structural OCT evaluation of glaucoma has focused on the tissue layers that are primarily affected by glaucoma, which include the NFL in the peripapillary region and the ganglion cell complex in the macula. The expectation is that OCTA evaluation should focus on the blood vessels supplying these layers in order to optimize glaucoma diagnosis and monitoring. However, it is wise to confirm this theoretical expectation with actual clinical data. An impediment to layer-by-layer analysis in OCT is the projection artifact,<sup>12</sup> which projects duplicates superficial blood vessels in deeper layers. Fortunately, it is possible to resolve the ambiguity between in-situ and projected vessels in deeper layers in post-processing using the PR-OCTA algorithm.<sup>12, 28, 29, 42, 43</sup> In a recent publication, we reported that in the macula, glaucoma primarily affects the SVC, and using the SVC slab, as opposed to the other deeper slabs, provides the best diagnostic accuracy and correlation with VF.<sup>25</sup> In this paper, we used the same technique to investigate the peripapillary region.

Based on our previous findings in the macular region, we anticipated that in the peripapillary region, both the NFLP and GCLP would be affected by glaucoma. We were surprised to find that the CD was significantly reduced only in the NFLP and not in the GCLP. Since we know that glaucoma causes loss of ganglion cells and the GCLP supplies the ganglion cell bodies,<sup>34, 44</sup> the disease should eventually affect the GCLP not only in the macula, but in the peripapillary region as well. Moreover, a recent study showed the progressive macular ganglion cell-inner plexiform layer thinning was detected most frequently in the inferotemporal region, then extended toward the fovea and optic disc.<sup>45</sup> Thus the most likely explanation for our finding is that the ganglion cell layer in the peripapillary region is affected primarily in the later stages of glaucoma. This explanation is also supported by the fact that the moderate-to-advanced glaucoma subgroup had lower GCLP-CD that was almost statistically significant – a larger sample of advanced glaucoma subjects is needed to test this hypothesis. The combination of NFLP and GCLP into SVC provided similar diagnostic accuracy and VF correlation as NFLP alone. And as the GCLP was often very thin, combining the two seemed more practical and served well for the analysis of glaucoma parameters in the peripapillary region. Therefore, both NFLP and SVC are good choices for glaucoma evaluation in the peripapillary region.

By using our compensation algorithm, NFLP-CD and SVC-CD were independent of SSI, but GCLP-CD, DVC-CD and all-plexus-CD were still positively correlated to SSI. Fortunately, the GCLP, DVC and all-plexus slabs were not affected by glaucoma, so this limitation didn't impact the glaucoma evaluation. Previous studies have shown the uncompensated VD or CD were correlated with SSI.<sup>25, 37, 46</sup> Since glaucoma group tended to have lower SSI, the compensation is necessary. Moreover, we can not rule out the age attenuation effect on the CD even if there were no significant changes. With the standard



deviation of the slope between age and CD, our sample size was too small to detect any significantly slow change.

We found the DVC, which included the ICP and DCP, to be minimally affected by glaucoma; which is what would be expected given that the DVC supplies the middle retinal layers that do not include the retinal ganglion cells. These results are in agreement with our PR-OCTA results in the macula, which also showed no DVC loss in glaucoma.<sup>25</sup>

Since the DVC is minimally affected by glaucoma, selectively measuring the SVC or NFLP slabs might be better than measuring all retinal plexuses. Our results supported this. SVC-CD and NFLP-CD offered better diagnostic accuracy and correlation with VF-MD compared to all-plexus CD. Furthermore, en face OCTA of the NFLP slab allowed the best visualization of focal glaucomatous defects. Therefore, we conclude that for glaucoma evaluation, the SVC or NFLP slabs should be used when analyzing OCTA; the deeper plexuses can be excluded. Since the NFLP and the SVC are the most superficial slabs, there are no projection artifacts in them, unlike the deeper ICP and DCP. Therefore both PR-OCTA and non-PR-OCTA provide equivalent results for NFLP-CD and SVC-CD. Thus although PR-OCTA was useful in determining which retinal plexuses are affected by glaucoma, both PR-OCTA and non-PR-OCTA work well for clinical glaucoma evaluation.

This OCTA quantitative retinal perfusion study agreed with previous case reports on the effects of retinal circulation in glaucoma. In 1968, Kornzweig et al found a postmortem eye with chronic glaucoma showing selective atrophy of the radial peripapillary capillaries (RPC), but the deeper capillaries appeared normal.<sup>47</sup> Recently, by using speckle variance OCTA, Mammo et al. found the density and morphologic characteristics of deeper capillary networks at the sites of RPC loss appeared normal in one glaucomatous eye.<sup>48</sup>

The nerve fiber layer plexus (NFLP) was traditionally known as the radial peripapillary capillaries (RPC). We are adopting the new term NFLP because wide-field OCT showed that the capillaries supplying the NFL are not limited to the immediate peripapillary region, but extend past the macula along the arcuate nerve fiber bundles.<sup>49</sup> Along these bundles, the orientation of the capillaries is parallel to the nerve fibers, which are arcuate rather than radial. Therefore the traditional term RPC is only appropriate for the small circumferential portion of the NFLP surrounding the optic disc. The new term NFLP is more thus appropriate.

Further refinement the VD measure, which includes capillaries and the larger vessels, compared to a measure of the capillaries alone, may improve its performance. Our results showed that CD offered slightly better diagnostic accuracy than VD, but both had excellent performance. The comparisons in this paper were based on overall global averages of the peripapillary retinal region. The next step in the development of OCTA analysis will be to divide the peripapillary region into sectors which will provide more specific information based on the peripapillary location of glaucoma damage. Theoretically, CD would have an advantage in sectoral analysis because it removes the noise introduced by variations in the pattern of large retinal vessels. Combining these empirical and theoretical considerations, we

believe CD may be better than VD for glaucoma evaluation. However, in their current forms, both parameters offer similar information.

We also compared traditional structural measures with OCTA parameters in glaucoma evaluation. Both NFLP-CD and SVC-CD had significantly stronger linear correlations with VF-MD than that between NFL thickness and VF-MD (Figure 4). No significant differences were found comparing the diagnostic power among NFLP-CD, SVC-CD and NFL thickness (Table 3). These findings were in agreement with the previous studies. Yarmohammadi et al. found peripapillary NFLP-VD had significantly stronger association with VF-MD than that between NFL thickness and VF-MD,<sup>14</sup> but OCTA parameters had similar diagnostic accuracy compared to NFL thickness for differentiating between healthy and glaucoma eyes.<sup>24</sup> In our first OCTA study of the peripapillary retina, we also showed that peripapillary retinal vessel density had better correlation with glaucoma severity than NFL thickness.<sup>21</sup> Overall OCTA perfusion parameters consistently show superior correlation with VF parameters, and may a better surrogate for VF function and a metric for monitoring glaucoma disease progression.

### Study Limitations

There are several limitations to our study. First, the relatively small sample size does not allow the detection of small differences in diagnostic accuracy. Second, the cross-sectional nature of the study does not allow any direct conclusions regarding utility in monitoring or predicting glaucoma progression. Third, most of the glaucoma participants were at early to moderate stages of disease, with only one in the advanced category. Thus we are not able to make conclusions as to which OCTA parameter may have better correlation with VF in advanced glaucoma. Fourth, participants with pre-perimetric glaucoma and glaucoma suspects were not included. Thus we could not make conclusions on the diagnostic accuracy in the earliest stages of glaucoma. Fifth, our study was not designed to contrast the potential differences between different types of glaucoma, or the potential effects of medications. Although our results suggest that the effects of both glaucoma eye drops and systemic medications are too small to be detected with our sample size and study design.

### Conclusions

In summary, we showed that OCTA evaluation of the peripapillary retina could measure CD and VD with tight population variation and high repeatability in normal and glaucoma participants. The NFLP slab provided the best diagnostic accuracy and the best contrast for visualizing focal peripapillary perfusion defects, while the SVC slab provided the best correlation with VF.

Further evaluation of OCTA technology for glaucoma evaluation is best served by focusing on these two slabs rather than deeper slabs or overall retinal circulation. We again demonstrated that perfusion parameters outperformed structural parameters in terms of correlation with VF, and therefore may possibly serve as a better surrogate for function and a better metric for monitoring glaucoma progression.

## Acknowledgement/Disclosure

### Funding/Support

Supported by NIH grants R01 EY023285, R01 EY010145, P30 EY010572, by unrestricted departmental funding from Research to Prevent Blindness (New York, NY) and the Champalimaud Foundation (Lisbon, Portugal). The sponsor or funding organization had no role in the design or conduct of this research.

## References

1. Quigley HA, Broman AT. The number of people with glaucoma worldwide in 2010 and 2020. *The British journal of ophthalmology* 2006;90:262–7. [PubMed: 16488940]
2. Congdon N, O'Colmain B, Klaver CC, et al. Causes and prevalence of visual impairment among adults in the United States. *Arch Ophthalmol* 2004;122:477–85. [PubMed: 15078664]
3. Friedman DS, Wolfs RC, O'Colmain BJ, et al. Prevalence of open-angle glaucoma among adults in the United States. *Arch Ophthalmol* 2004;122:532–8. [PubMed: 15078671]
4. Gupta P, Zhao D, Guallar E, Ko F, Boland MV, Friedman DS. Prevalence of Glaucoma in the United States: The 2005-2008 National Health and Nutrition Examination Survey. *Invest Ophthalmol Vis Sci* 2016;57:2905–2913. [PubMed: 27168366]
5. Mwanza JC, Oakley JD, Budenz DL, Anderson DR, Cirrus Optical Coherence Tomography Normative Database Study G. Ability of cirrus HD-OCT optic nerve head parameters to discriminate normal from glaucomatous eyes. *Ophthalmology* 2011;118:241–8 e1. [PubMed: 20920824]
6. Medeiros FA, Zangwill LM, Bowd C, Vessani RM, Susanna R Jr., Weinreb RN. Evaluation of retinal nerve fiber layer, optic nerve head, and macular thickness measurements for glaucoma detection using optical coherence tomography. *American journal of ophthalmology* 2005;139:44–55. [PubMed: 15652827]
7. Schuman JS, Hee MR, Puliafito CA, et al. Quantification of nerve fiber layer thickness in normal and glaucomatous eyes using optical coherence tomography. *Arch Ophthalmol* 1995;113:586–96. [PubMed: 7748128]
8. Guedes V, Schuman JS, Hertzmark E, et al. Optical coherence tomography measurement of macular and nerve fiber layer thickness in normal and glaucomatous human eyes. *Ophthalmology* 2003;110:177–89. [PubMed: 12511364]
9. Mwanza JC, Durbin MK, Budenz DL, et al. Glaucoma diagnostic accuracy of ganglion cell-inner plexiform layer thickness: comparison with nerve fiber layer and optic nerve head. *Ophthalmology* 2012;119:1151–8. [PubMed: 22365056]
10. Tan O, Chopra V, Lu AT, et al. Detection of macular ganglion cell loss in glaucoma by Fourier-domain optical coherence tomography. *Ophthalmology* 2009;116:2305–14 e1–2. [PubMed: 19744726]
11. Tan O, Li G, Lu AT, Varma R, Huang D, Advanced Imaging for Glaucoma Study G. Mapping of macular substructures with optical coherence tomography for glaucoma diagnosis. *Ophthalmology* 2008;115:949–56. [PubMed: 17981334]
12. Zhang M, Hwang TS, Campbell JP, et al. Projection-resolved optical coherence tomographic angiography. *Biomed Opt Express* 2016;7:816–28. [PubMed: 27231591]
13. Wollstein G, Kagemann L, Bilonick RA, et al. Retinal nerve fibre layer and visual function loss in glaucoma: the tipping point. *The British journal of ophthalmology* 2012;96:47–52. [PubMed: 21478200]
14. Yarmohammadi A, Zangwill LM, Diniz-Filho A, et al. Relationship between Optical Coherence Tomography Angiography Vessel Density and Severity of Visual Field Loss in Glaucoma. *Ophthalmology* 2016;123:2498–2508. [PubMed: 27726964]
15. Bowd C, Zangwill LM, Weinreb RN, Medeiros FA, Belghith A. Estimating Optical Coherence Tomography Structural Measurement Floors to Improve Detection of Progression in Advanced Glaucoma. *American journal of ophthalmology* 2017;175:37–44. [PubMed: 27914978]

16. Ajtony C, Balla Z, Somoskeoy S, Kovacs B. Relationship between visual field sensitivity and retinal nerve fiber layer thickness as measured by optical coherence tomography. *Invest Ophthalmol Vis Sci* 2007;48:258–63. [PubMed: 17197541]
17. Hood DC, Kardon RH. A framework for comparing structural and functional measures of glaucomatous damage. *Prog Retin Eye Res* 2007;26:688–710. [PubMed: 17889587]
18. Jia Y, Tan O, Tokayer J, et al. Split-spectrum amplitude-decorrelation angiography with optical coherence tomography. *Opt Express* 2012;20:4710–25. [PubMed: 22418228]
19. Jia Y, Morrison JC, Tokayer J, et al. Quantitative OCT angiography of optic nerve head blood flow. *Biomed Opt Express* 2012;3:3127–37. [PubMed: 23243564]
20. Jia Y, Wei E, Wang X, et al. Optical Coherence Tomography Angiography of Optic Disc Perfusion in Glaucoma. *Ophthalmology* 2014;121:1322–1332. [PubMed: 24629312]
21. Liu L, Jia Y, Takusagawa HL, et al. Optical Coherence Tomography Angiography of the Peripapillary Retina in Glaucoma. *JAMA Ophthalmol* 2015;133:1045–52. [PubMed: 26203793]
22. Chen CL, Zhang A, Bojikian KD, et al. Peripapillary Retinal Nerve Fiber Layer Vascular Microcirculation in Glaucoma Using Optical Coherence Tomography-Based Microangiography. *Invest Ophthalmol Vis Sci* 2016;57:OCT475–85. [PubMed: 27442341]
23. Chen CL, Bojikian KD, Wen JC, et al. Peripapillary Retinal Nerve Fiber Layer Vascular Microcirculation in Eyes With Glaucoma and Single-Hemifield Visual Field Loss. *JAMA Ophthalmol* 2017;135:461–468. [PubMed: 28358939]
24. Yarmohammadi A, Zangwill LM, Diniz-Filho A, et al. Optical Coherence Tomography Angiography Vessel Density in Healthy, Glaucoma Suspect, and Glaucoma Eyes. *Invest Ophthalmol Vis Sci* 2016;57:OCT451–9. [PubMed: 27409505]
25. Takusagawa HL, Liu L, Ma KN, et al. Projection-Resolved Optical Coherence Tomography Angiography of Macular Retinal Circulation in Glaucoma. *Ophthalmology* 2017;124:1589–1599. [PubMed: 28676279]
26. Yarmohammadi A, Zangwill LM, Manalastas PIC, et al. Peripapillary and Macular Vessel Density in Patients with Primary Open-Angle Glaucoma and Unilateral Visual Field Loss. *Ophthalmology* 2018;125:578–587. [PubMed: 29174012]
27. Wang J, Zhang M, Hwang TS, et al. Reflectance-based projection-resolved optical coherence tomography angiography [Invited]. *Biomed Opt Express* 2017;8:1536–1548. [PubMed: 28663848]
28. Campbell JP, Zhang M, Hwang TS, et al. Detailed Vascular Anatomy of the Human Retina by Projection-Resolved Optical Coherence Tomography Angiography. *Sci Rep* 2017;7:42201. [PubMed: 28186181]
29. Patel RC, Wang J, Hwang TS, et al. Plexus-Specific Detection of Retinal Vascular Pathologic Conditions with Projection-Resolved OCT Angiography. *Ophthalmol Retina* 2018;2:816–826. [PubMed: 30148244]
30. Kraus MF, Potsaid B, Mayer MA, et al. Motion correction in optical coherence tomography volumes on a per A-scan basis using orthogonal scan patterns. *Biomed Opt Express* 2012;3:1182–99. [PubMed: 22741067]
31. Zhang M, Wang J, Pechauer AD, et al. Advanced image processing for optical coherence tomographic angiography of macular diseases. *Biomed Opt Express* 2015;6:4661–75. [PubMed: 26713185]
32. Yali Jia SG, David Huang Chapter 5: Artifacts in Optical Coherence Tomography Angiography *Optical Coherence Tomography Angiography of the Eye*. Thorofare, NJ, USA: SLACK Incorporated, 2017.
33. Snodderly DM, Weinhaus RS, Choi JC. Neural-vascular relationships in central retina of macaque monkeys (*Macaca fascicularis*). *J Neurosci* 1992;12:1169–93. [PubMed: 1556592]
34. Provis JM. Development of the primate retinal vasculature. *Prog Retin Eye Res* 2001;20:799–821. [PubMed: 11587918]
35. Snodderly DM, Weinhaus RS. Retinal vasculature of the fovea of the squirrel monkey, *Saimiri sciureus*: three-dimensional architecture, visual screening, and relationships to the neuronal layers. *J Comp Neurol* 1990;297:145–63. [PubMed: 2376631]

36. Yali Jia BL, Simon Gao, David Huang. Chapter 3: Cross-Sectional and En Face Visualization of Posterior Eye Circulations Optical Coherence Tomography Angiography of the Eye. Thorofare, NJ, USA: SLACK Incorporated, 2017.
37. Gao SS, Jia Y, Liu L, et al. Compensation for Reflectance Variation in Vessel Density Quantification by Optical Coherence Tomography Angiography. *Invest Ophthalmol Vis Sci* 2016;57:4485–92. [PubMed: 27571015]
38. Diedenhofen B, Musch J. cocor: a comprehensive solution for the statistical comparison of correlations. *PLoS One* 2015;10:e0121945. [PubMed: 25835001]
39. Zhou X-H, McClish DK, Obuchowski NA. *Statistical methods in diagnostic medicine*: John Wiley & Sons, 2009.
40. DeLong ER, DeLong DM, Clarke-Pearson DL. Comparing the areas under two or more correlated receiver operating characteristic curves: a nonparametric approach. *Biometrics* 1988;44:837–45. [PubMed: 3203132]
41. Hodapp EPRI, Anderson DR. *Clinical decisions in glaucoma*. St Louis: The CV Mosby Co 1993;pp. 52–61.
42. Hwang TS, Hagag AM, Wang J, et al. Automated Quantification of Nonperfusion Areas in 3 Vascular Plexuses With Optical Coherence Tomography Angiography in Eyes of Patients With Diabetes. *JAMA Ophthalmol* 2018;136:929–936. [PubMed: 29902297]
43. Patel R, Wang J, Campbell JP, et al. Classification of Choroidal Neovascularization Using Projection-Resolved Optical Coherence Tomographic Angiography. *Investigative Ophthalmology & Visual Science* 2018;59:4285–4291. [PubMed: 30372757]
44. Snodderly DM, Weinhaus RS, Choi JC. Neural-vascular relationships in central retina of macaque monkeys (*Macaca fascicularis*). *J Neurosci* 1992;12:1169–93. [PubMed: 1556592]
45. Shin JW, Sung KR, Park SW. Patterns of Progressive Ganglion Cell-Inner Plexiform Layer Thinning in Glaucoma Detected by OCT. *Ophthalmology* 2018;125:1515–1525. [PubMed: 29705057]
46. Rao HL, Pradhan ZS, Weinreb RN, et al. Determinants of Peripapillary and Macular Vessel Densities Measured by Optical Coherence Tomography Angiography in Normal Eyes. *Journal of glaucoma* 2017;26:491–497. [PubMed: 28263261]
47. Kornzweig AL, Eliasoph I, Feldstein M. Selective atrophy of the radial peripapillary capillaries in chronic glaucoma. *Arch Ophthalmol* 1968;80:696–702. [PubMed: 4177355]
48. Mammo Z, Heisler M, Balaratnasingam C, et al. Quantitative Optical Coherence Tomography Angiography of Radial Peripapillary Capillaries in Glaucoma, Glaucoma Suspect, and Normal Eyes. *American journal of ophthalmology* 2016;170:41–49. [PubMed: 27470061]
49. Jia Y, Simonett JM, Wang J, et al. Wide-Field OCT Angiography Investigation of the Relationship Between Radial Peripapillary Capillary Plexus Density and Nerve Fiber Layer Thickness. *Invest Ophthalmol Vis Sci* 2017;58:5188–5194. [PubMed: 29049718]

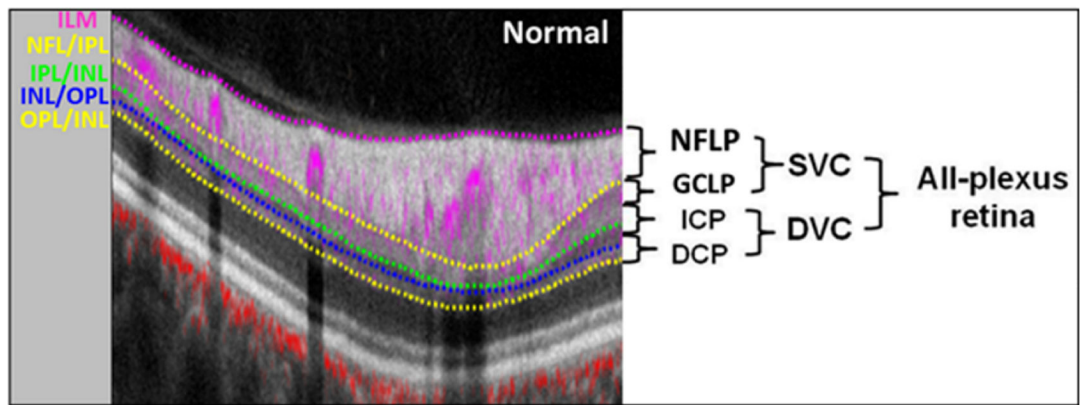


**Figure 1.**

Relationship between the retinal vascular plexuses and anatomic layers. Cross-sectional projection-resolved optical coherence tomography angiograms (PR-OCTA) of a normal eye. The 4.5-mm section was taken 1-mm superior to the center of the disc. Flow signals (purple for retinal and red for choroidal blood flow) were overlaid on reflectance signal (gray scale). ILM = inner limiting membrane, NFL = nerve fiber layer, GCL = ganglion cell layer, IPL = inner plexiform layer, INL = inner nuclear layer, OPL = outer plexiform layer, ONL = outer nuclear layer, NFLP = nerve fiber layer plexus, GCLP = ganglion cell layer plexus (inner 80% of GCC excluding NFLP), SVC = superficial vascular complex (inner 80% of GCC), ICP = intermediate capillary plexus (outer 20% of GCC + inner 50% of INL), DCP = deep capillary plexus (outer 50% of INL + OPL), DVC = deep vascular complex (ICP + DCP).



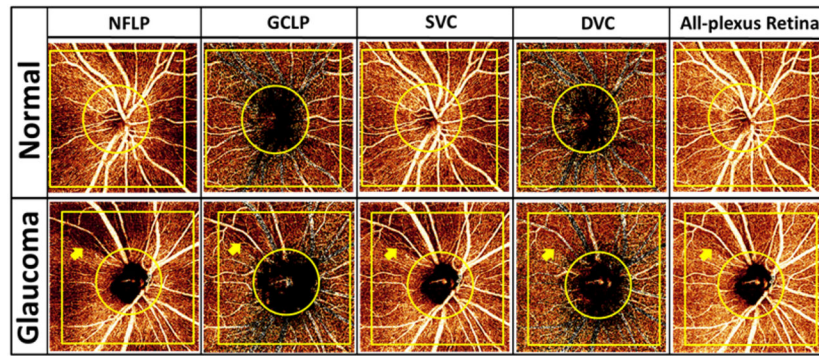


**Figure 2.**

Comparison between a normal eye (top 5 panels) and a perimetric glaucoma eye (bottom 5 panels). The angiograms shown are 4.5×4.5 mm *en face* projection-resolved optical coherence tomography angiography (PR-OCTA). The focal capillary dropout in the glaucomatous eye (arrow) could be visualized more clearly in the nerve fiber layer plexus (NFLP) slab than on the ganglion cell layer plexus (GCLP), superficial vascular complex (SVC) and all-plexus retinal angiograms, while the deep vascular complex (DVC) appeared unaffected. The capillary density (CD) was calculated in the 4×4 mm yellow square excluding a 2mm diameter circle centered on the optic disc.

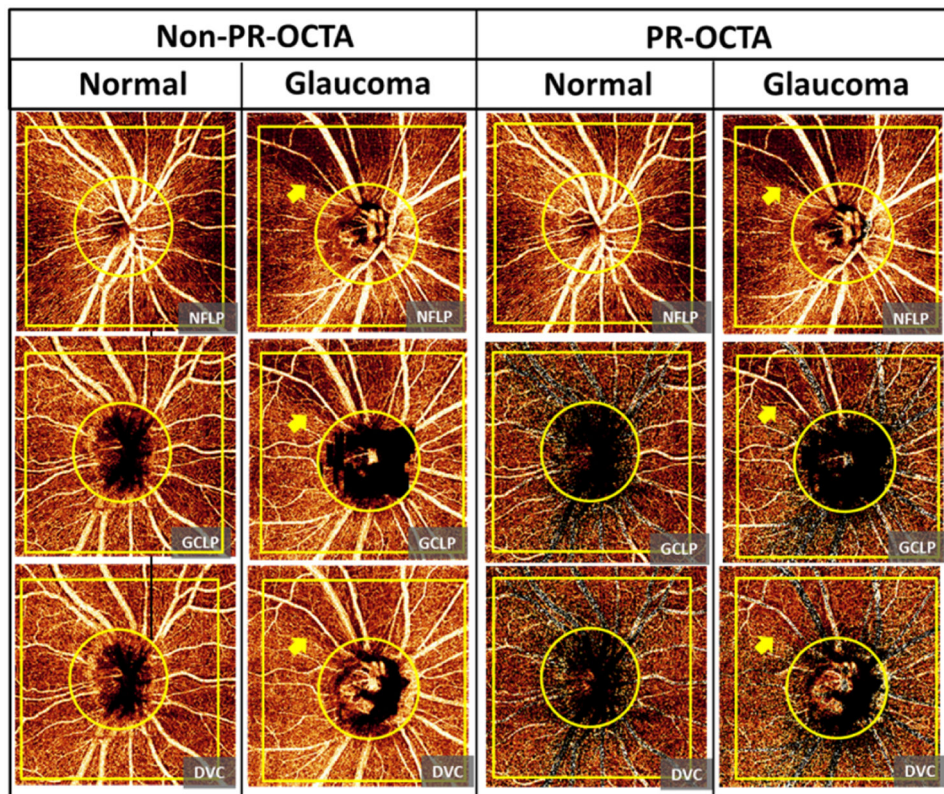


**Figure 3.**

Comparison of the ganglion cell layer plexus (GCLP) and the deep vascular complex (DVC) angiograms between non projection-resolved optical coherence tomography angiography (non-PR-OCTA) and PR-OCTA from a normal eye and a perimetric glaucoma eye. The vessel pattern in the nerve fiber layer plexus (NFLP), large vessels and radial capillaries, were projected in the non-PR-OCTA GCLP and DVC angiograms in both normal and glaucoma eyes. PR-OCTA removed these projected patterns in the GCLP and DVC angiograms. The non-PR-OCTA DVC angiogram showed projected perfusion defects (arrow) in the glaucoma eye. The PR-OCTA showed that the DVC was unaffected by glaucoma.

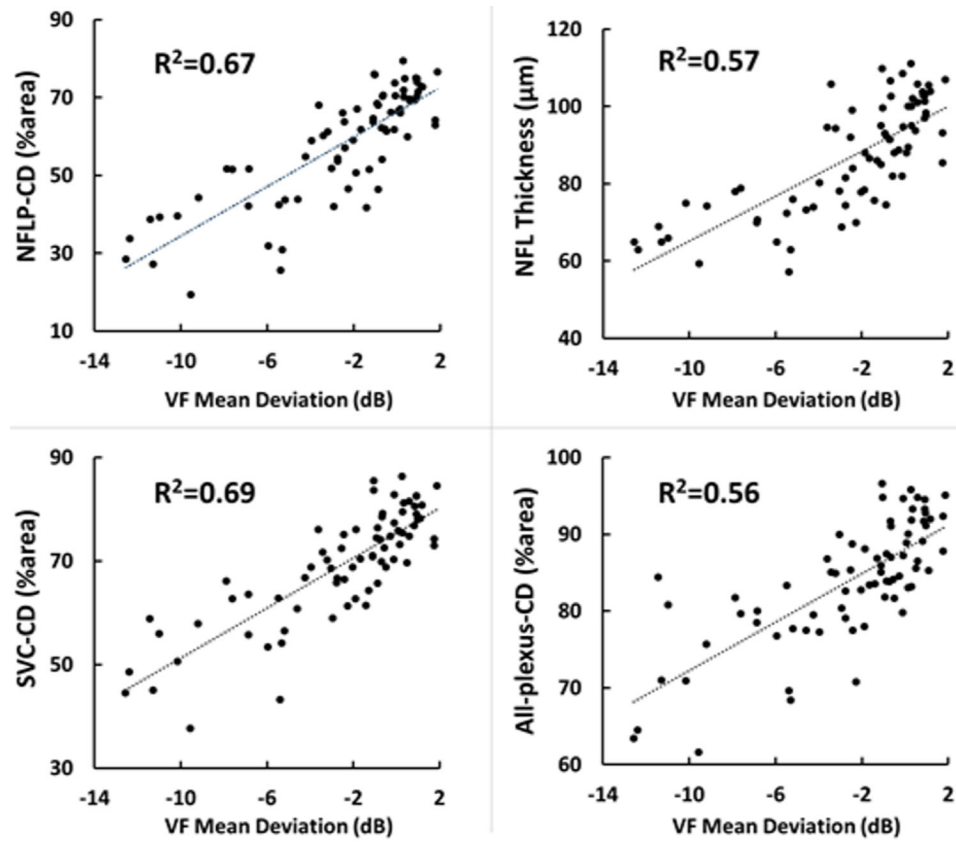


**Figure 4.** Scatterplots illustrating the linear correlation between visual field (VF) mean deviation and peripapillary retinal measurements by structural optical coherence tomography (OCT) and OCT angiography. CD=capillary density, NFLP= nerve fiber layer plexus, NFL=nerve fiber layer, SVC=superficial vascular complex.

**Table 1.**

## Participants' Characteristics

Parameter	Normal	Glaucoma	Mean Difference (95% CI, P value)	
Participants, n	34	41		
Eyes, n	34	41		
Age (Years)	65.3 ± 8.9	64.9 ± 9.3	-0.4 (-4.8~ 4.0, 0.853)	
Glaucoma drops. n (%)	0 (0%)	1.9 ± 0.8,41 (100%)		
Intraocular Pressure (mm Hg)	14.9 ± 3.6	15.1 ± 2.7	0.2 (-1.2~ 1.7, 0.767)	
Axial Length (mm)	23.9 ± 1.2	24.3 ± 1.1	0.4 (-0.1~ 1.0, 0.830)	
Diastolic Blood Pressure (mm Hg)	76.1 ± 16.0	77.4 ± 10.9	1.3 (-5.4~ 7.9, 0.702)	
Systolic Blood Pressure (mm Hg)	121.9 ± 25.2	126.2 ± 15.9	4.3 (-6.1~ 14.5, 0.415)	
Mean Ocular Perfusion Pressure (mm Hg)	46.1 ± 10.2	47.3 ± 6.9	1.3 (-3.0~ 5.4, 0.562)	
<b>Visual Field</b>	MD (dB)	0.06 ± 1.16 (-3.22 ~ 1.87)	-4.77 ± 3.70 (-12.56~ -0.12)	-4.83 (-6.3~ -3.7, <0.001)
	PSD (dB)	1.42 ± 0.25 (1.02 ~ 2.17)	6.20 ± 3.90 (1.51 ~ 14.24)	4.78 (3.7~ 6.4, <0.001)
<b>Structural OCT Thickness Measurement</b>	NFL (µm)	97.9 ± 7.0 (85~111)	77.5 ± 11.8 (57 ~100)	-20.4 (-25.0~ -15.8, <0.001)
	Signal Strength Index	69 ± 8 (54~89)	64 ± 8 (50~84)	-5 (-9~ -1, <0.001)
	NFLP-CD	69.4 ± 4.8 (59.9~79.6)	48.5 ± 12.9 (19.1~76.1)	-20.9 (-25.2~16.2, <0.001)
	GCLP-CD	49.4 ± 5.6 (39.5~62.1)	48.5 ± 5.5 (37.5~60.1)	-0.9 (-3.5~ 1.7, 0.477)
<b>OCT Angiography Measurements (% area)</b>	SVC-CD	77.4 ± 4.3 (69.7~86.3)	62.4 ± 9.9 (37.4~85.5)	-15.0 (-18.6~ -11.5, <0.001)
	DVC-CD	48.4 ± 9.3 (29.4~65.1)	48.5 ± 9.8 (29.6~66.8)	0.1 (-4.3~ 4.4, 0.977)
	All-Plexus-CD	89.3 ± 4.0 (83.0~95.8)	79.4 ± 7.4 (58.7~96.6)	-9.9 (-12.6~ -6.9, <0.001)
	NFLP-VD	75.7 ± 4.2 (67.0~83.9)	57.6 ± 11.7 (33.0~82.1)	-18.1 (-22.4~ -13.9, <0.001)
SVC-VD	82.5 ± 3.7 (75.8~89.5)	70.2 ± 8.6 (49.2~89.8)	-12.3 (-15.5~ -9.2, <0.001)	

Numbers displayed are mean ± standard deviation (range); CI = confidence interval, MD = mean deviation, PSD = pattern standard deviation, NFL = nerve fiber layer, CD = capillary density, VD = vessel density, NFLP = nerve fiber layer plexus, GCLP = ganglion cell layer plexus, SVC = superficial vascular complex, DVC = deep vascular complex.

**Table 2.**

Repeatability and Normal Population Variability of Peripapillary Retinal Optical Coherence Tomography Angiographic Parameters

Group	Normal (N=34)		Glaucoma (N=41)	All (N=75)
	Within-visit repeatability (Pooled SD)	Population variation (SD)	Within-visit repeatability (Pooled SD)	Intraclass correlation coefficient
NFLP-CD	2.0 % area	4.8% area	2.2 % area	0.981
GCLP-CD	2.0 % area	5.7% area	2.1 % area	0.880
SVC-CD	1.7 % area	4.3% area	1.9 % area	0.976
DVC-CD	3.2 % area	8.9% area	3.2 % area	0.889
All-Plexus-CD	1.0 % area	3.9% area	1.7 % area	0.974

SD = standard deviation; CD = capillary density, NFLP = nerve fiber layer plexus, GCLP = ganglion cell layer plexus, SVC = superficial vascular complex, DVC = deep vascular complex.

**Table 3.**

Diagnostic Accuracy of Peripapillary Retinal Optical Coherence Tomography Angiographic and Structural Parameters

Parameters	AROC	Sensitivity* (95% confidence interval)
NFLP-CD	0.947	90.2% (76.9%~97.2%)
GCLP-CD	0.549	9.8% (2.8%~23.1%)
SVC-CD	0.942	85.3% (70.8%~94.4%)
DVC-CD	0.509	4.9% (0.7%~16.6%)
All-Plexus-CD	0.893	73.2% (57.1%~85.8%)
NFL thickness	0.918	82.9% (67.9%~92.8%)

\* Sensitivities at 95% specificity were evaluated. AROC=area under the receiver operating characteristic curve, CD = capillary density, NFL = nerve fiber layer, NFLP = nerve fiber layer plexus, GCLP = ganglion cell layer plexus, SVC = superficial vascular complex, DVC = deep vascular complex.

Author Manuscript

Author Manuscript

Author Manuscript

Author Manuscript



**Table 4.**

Correlation Matrix of Visual Field, Peripapillary Retinal Optical Coherence Tomography Angiographic and Structural Parameters

Parameters	NFLP-CD	GCLP-CD	SVC-CD	DVC-CD	All-plexus-CD	NFL thickness
GCLP-CD	0.218(0.060)					
SVC-CD	<b>0.979(0.000)</b>	<b>0.404(0.000)</b>				
DVC-CD	-0.088(0.455)	<b>0.754(0.000)</b>	0.011(0.924)			
All-plexus-CD	<b>0.853(0.000)</b>	<b>0.609(0.000)</b>	<b>0.910(0.000)</b>	<b>0.397(0.000)</b>		
NFL Thickness	<b>0.926(0.000)</b>	<b>0.285(0.012)</b>	<b>0.914(0.000)</b>	0.020(0.863)	<b>0.837(0.000)</b>	
VF-MD	<b>0.819(0.000)</b>	<b>0.275(0.017)</b>	<b>0.831(0.000)</b>	-0.029(0.808)	<b>0.750(0.000)</b>	<b>0.759(0.000)</b>

Pearson's r (p-value); Statistically significant correlation ( $p < 0.05$ ) are bold faced. CD=capillary density, NFL = nerve fiber layer, NFLP = nerve fiber layer plexus, GCLP = ganglion cell layer plexus, SVC = superficial vascular complex, DVC = deep vascular complex, VF-MD= visual field mean deviation.

**Table 5.**

Comparison of the Performance of Capillary Density and Vessel Density in Nerve Fiber Layer Plexus and Superficial Vascular Complex Slabs

Parameters	Normal (N=34)		Glaucoma (N=41)	ALL (N=75)		
	Within-visit repeatability (Pooled SD)	Population variation (SD)	Within-visit repeatability (Pooled SD)	ICC	Correlation with VF-MD (dB)	AROC
NFLP-CD	2.0 % area	4.8% area	2.2 % area	0.981	0.819	0.947
NFLP-VD	1.9 % area	4.2% area	2.3 % area	0.977	0.828	0.934
SVC-CD	1.7 % area	4.3% area	1.9 % area	0.976	0.831	0.942
SVC-VD	1.6 % area	3.7% area	1.8 % area	0.970	0.830	0.919

CD=capillary density, VD = vessel density, NFL = nerve fiber layer, NFLP = nerve fiber layer plexus, SVC = superficial vascular complex, VF-MD = visual field mean deviation. ICC = Intraclass correlation coefficient, AROC=area under the receiver operating characteristic curve.